

2022

Impact of voids and backfill on seismic wave velocity-preliminary results

Author(s) ORCID Identifier:

Zarina Mukhamedyarova:  0000-0002-3056-8110

Fidelis Suorineni:  0000-0002-7356-5446

Temirlan Aldubay:  0000-0002-1728-7920

Gylym Sapinov:  0000-0002-1853-6810

Follow this and additional works at: <https://jsm.gig.eu/journal-of-sustainable-mining>



Part of the [Explosives Engineering Commons](#), [Oil, Gas, and Energy Commons](#), and the [Sustainability Commons](#)

Recommended Citation

Mukhamedyarova, Zarina; Suorineni, Fidelis; Aldubay, Temirlan; and Sapinov, Gylym (2022) "Impact of voids and backfill on seismic wave velocity-preliminary results," *Journal of Sustainable Mining*: Vol. 21 : Iss. 4 , Article 7.

Available at: <https://doi.org/10.46873/2300-3960.1370>

This Research Article is brought to you for free and open access by Journal of Sustainable Mining. It has been accepted for inclusion in Journal of Sustainable Mining by an authorized editor of Journal of Sustainable Mining.

Impact of voids and backfill on seismic wave velocity-preliminary results

Abstract

In this study, laboratory experiments were conducted on discrete physical models that mimic mining effects to better understand the impact of continuous changes in mining environments on seismic wave velocities. The discrete physical models are represented by concrete and granite cubic samples of different sizes with holes of different diameters filled and unfilled with cemented sand backfill of different cement-sand content ratios. The hole diameters range from 0 to 150 mm in block sizes ranging from 150 mm to 450 mm in increments of 75 mm. The increasing hole size mimics increasing extraction in the mine with time. Cemented sand fills at cement contents ranging from 0 to 20% are used to fill the voids after testing them empty and retesting the same at different backfill cured ages. The SAEU3H AE eight-channel system is used in the study. Preliminary results show that the impact of continuous changes in mining environments significantly affects the seismic wave velocities. The impact of voids and their contents on the seismic wave velocity depends on the sensor location relative to source and void, and its backfills cement content with time.

Keywords

seismic event source location accuracy, constantly changing mine conditions, real-time seismic wave velocity, void and cemented sand backfill effect with time

Creative Commons License



This work is licensed under a [Creative Commons Attribution-Noncommercial-No Derivative Works 4.0 License](https://creativecommons.org/licenses/by-nc-nd/4.0/).

Impact of Voids and Backfill on Seismic Wave Velocity-Preliminary Results

Zarina Mukhamedyarova ^a, Fidelis Suorineni ^{a,*}, Temirlan Aldubay ^a, Gylym Sapinov ^b

^a Nazarbayev University, School of Mining and Geosciences, Nur-Sultan, Kazakhstan

^b Karaganda Technical University, Department of Development of Mineral Deposits, Karaganda, Kazakhstan

Abstract

In this study, laboratory experiments were conducted on discrete physical models that mimic mining effects to better understand the impact of continuous changes in mining environments on seismic wave velocities. The discrete physical models are represented by concrete and granite cubic samples of different sizes with holes of different diameters filled and unfilled with cemented sand backfill of different cement-sand content ratios. The hole diameters range from 0 to 150 mm in block sizes ranging from 150 mm to 450 mm in increments of 75 mm. The increasing hole size mimics increasing extraction in the mine with time. Cemented sand fills at cement contents ranging from 0 to 20% are used to fill the voids after testing them empty and retesting the same at different backfill cured ages. The SAEU3H AE eight-channel system is used in the study. Preliminary results show that the impact of continuous changes in mining environments significantly affects the seismic wave velocities. The impact of voids and their contents on the seismic wave velocity depends on the sensor location relative to source and void, and it backfills cement content with time.

Keywords: source location, changing ground condition, seismic wave velocity, discrete physical modelling

1. Introduction

With the increasing depletion and production of mineral resources, underground mines are going deeper worldwide. High in situ stresses coupled with a complex geological environment result in rock burst, rock mass failure, and excavation deformations [1–5].

Microseismic monitoring systems are integral parts of deep underground mining. These systems help to understand mining-induced seismicity to mitigate their potential hazards in predicted locations. However, microseismic monitoring system's accuracy in predicting the event source location depends on the input velocity in the event source calculation [6].

Recent research has identified that wave velocities in rock masses in underground mining are not

constant as previously often assumed in seismic monitoring systems source location algorithms. Rock masses in mining environments are continuously degraded because of mining. Hence the use of 3D velocity models based on 3D ray tracing in heterogeneous media that consider the presence of voids from mining activities is actively researched [7]. This approach shows some improvements in the accuracy of seismic event source locations. However, seismic wave velocity changes are not only due to the introduction of voids but also several other sources of rock mass degradation, including stress-induced fracturing and the state of the voids created, including their constantly changing size, shapes, and contents. Laboratory study of the seismic wave propagation through rock samples tracks properties such as sample heterogeneity and fracture intensity [8].

Abbreviations: AE, acoustic emission; UCS, uniaxial compressive strength; AET, acoustic emission technique; ASTM C-109 C, standard Test Method for Compressive Strength of Hydraulic Cement Mortars; ISRM, International Society for Rock Mechanics; μ , friction coefficient; ω_r , resonant frequency; m , mass; γ , seismic wave attenuation; Q , quality factor; CCVM, continuously changing velocity model; ϕ , diameter; CAMIRO, Canada Mining Innovation Research Organization,

Received 17 March 2022; revised 25 July 2022; accepted 27 July 2022.
Available online 23 November 2022

* Corresponding author.

E-mail address: fidelis.suorineni@nu.edu.kz (F. Suorineni).

<https://doi.org/10.46873/2300-3960.1370>

2300-3960/© Central Mining Institute, Katowice, Poland. This is an open-access article under the CC-BY 4.0 license (<https://creativecommons.org/licenses/by/4.0/>).

Seismic wave propagation is highly affected by rock mass structure and fluid content. Many pieces of research in recent years have shown that rock mass micro-fracturing is the critical factor affecting seismic wave velocity and attenuation. Therefore, it is crucial to understand the effect of attenuation on wave velocity due to rock mass fracturing [9].

This paper presents a novel approach and preliminary research results aimed at predicting wave velocities in real-time in the constantly changing underground mining conditions. The underground mine is challenging to control, while the laboratory is a perfect controlled condition to simulate and study seismicity. The driving force and interest in this research are to find solutions to the rockburst problem in the mining industry to improve safety and productivity. The novelty of the research is the use of discrete physical models as analogs to mimic the changing ground conditions in underground mining to capture the impact on seismic wave velocity.

In the discrete physical modelling concept, rather than using a single block and changing its condition to reflect the constantly changing ground condition in mining environments (a physically challenging approach), separate individual blocks are used with each block representing a different stage in the mining process in time, structure, and geometry.

2. Materials and methods

To understand changes in seismic wave velocity in constantly changing mining conditions, laboratory physical models that mimic constantly changing underground mining conditions were developed. The novel approach of using discrete physical models to solve a rather complex problem was strategically developed and executed in the laboratory to enable fundamental factors governing seismic wave velocity changes to be captured. This approach overcomes the complex mining environment that is somewhat more problematic to control.

2.1. Physical laboratory models mimicking the continuously changing underground mine environment

Rock (granite) and concrete block samples were used as the discrete mine models. Sample material choice was based on rock homogeneity. Sample sizes varied between 150 mm and 450 mm cubes at 75 mm side length increments (Fig. 1).

For each cube size, one cube had no hole, while another had a hole in its centre of a diameter depending on the cube size to account for the cube

boundary conditions. Hole diameters varied from 50 mm in the 150 mm cubes to 150 mm diameter in the 450 mm cube at increments of 25 mm, as shown in Table 1.

The increasing hole diameters mimicked the increasing extraction and the mine maturity with time. In principle, the increasing hole diameter in the blocks of increasing size represents the total amount of voids (sum of all voids in the mine with increasing maturity) in the mine with time.

In mining practice, voids such as stopes are usually filled with backfill of various types. To mimic backfilling, the holes in the blocks were subsequently filled with a backfill (Fig. 2) with different cement to sand ratios of 0, 5, 10, 15, and 20%. The 0% cement content backfill was tested dry and wet. Each 5–20% cement backfill was cured for 8 h, 1 day, 7 days, 14 days, and 28 days and tested to account for curing time impact on seismic wave velocity.

Initially, samples with holes were tested empty to represent a mine without a backfill. In the following tests, the holes were filled with different cement to sand ratio backfills cured for 8 h, 1 day, 7 days, 14 days, and 28 days to represent a mine with different backfill types and ages. Testing after 28 days of curing was chosen since concrete gains 99% strength after 28 days [10].

Each cube was attached with eight sensors for the wave velocity determination tests, one of which was used as a source (pulse) and the other seven as receivers of the seismic wave arrival times at known coordinate locations based on established grids on each cube (Fig. 3).

2.2. Materials

Granite and concrete cubes and backfill were used in the tests. The following sections describe the details of these materials.

2.2.1. Granite cubes

The study involves laboratory experiments with homogeneous rock samples of granite. Sample homogeneity was the critical factor for the choice of rock type. The surfaces of the cubes must be polished to a tolerance of 1 mm, with each opposite face parallel to each other. The homogeneity and isotropy of the rock allowed for the results to be comparable. It was a challenge to prepare granite cubes in-house to meet these specifications. Hence, a professional stone vendor was used.

Ideally, it was planned to use only the granite cubes for the project. However, the cost of the

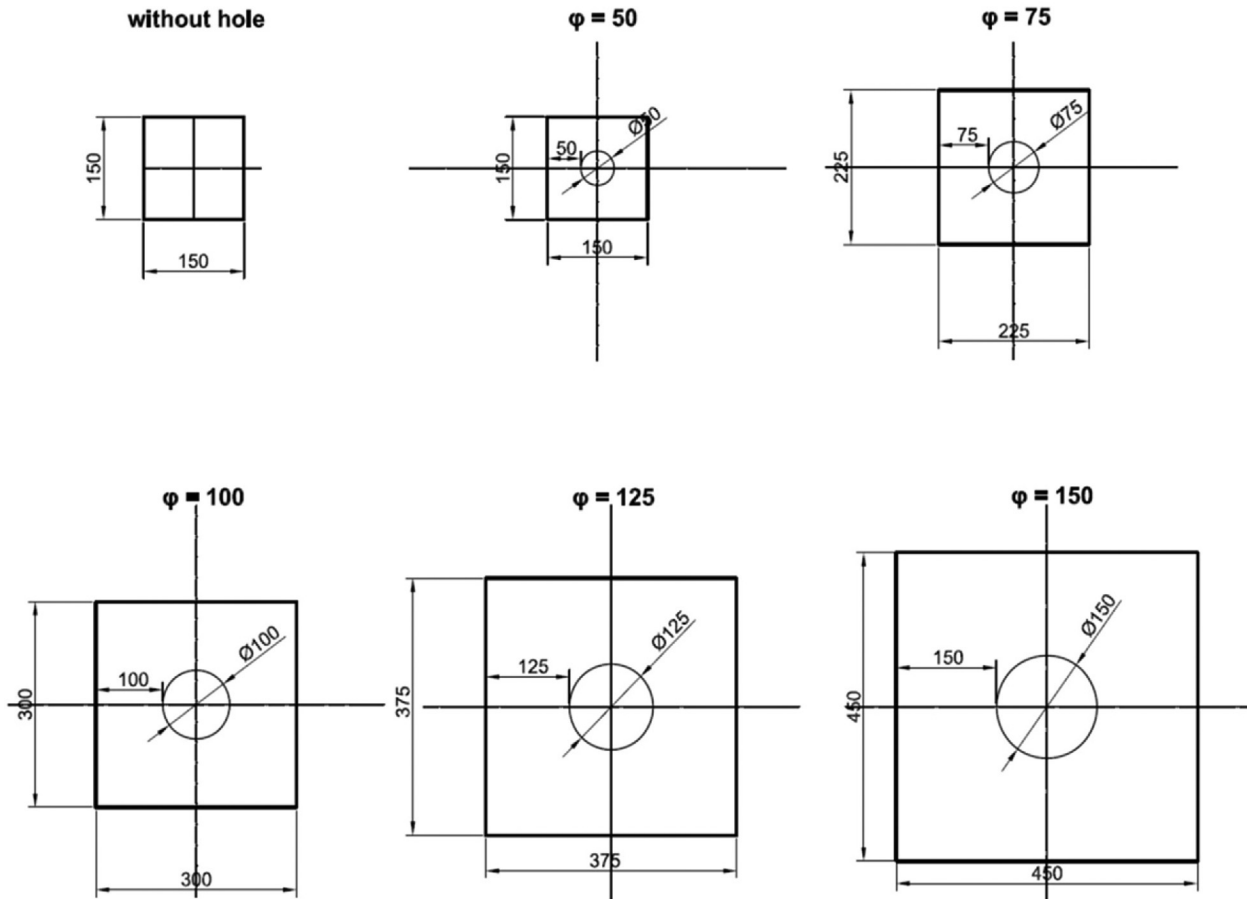


Fig. 1. Sample sizes varying between 150 and 450 mm cubes at 75 mm side length increments representing various stages of mining in time. Hole diameters represent increasing extraction with time.

granite cubes and the challenge of obtaining samples that were consistent in composition resulted in the use of synthetic rock in the form of concrete cubes.

2.2.2. Concrete cubes

The concrete cubes were moulded in the laboratory with a mixture of sand and cement to represent rock. A suitable cement to sand ratio was

established through the ASTM C-109 C standard [11]. The cubes were used after curing for 28 days. Material proportions for standard mortars according to ASTM C-109 C standard:

Table 1. Block sizes and hole diameters.

Cube size (mm)	Material type	Hole diameter (mm)
150	concrete	0 (no hole)
150	concrete	50
225	concrete	0 (no hole)
225	concrete	75
300	granite	0 (no hole)
300	granite	100
375	concrete	0 (no hole)
375	concrete	125
450	concrete	0 (no hole)
450	concrete	150



Fig. 2. Granite rock samples with a cube size of 300 mm with and without holes (hole diameter is 100 mm).

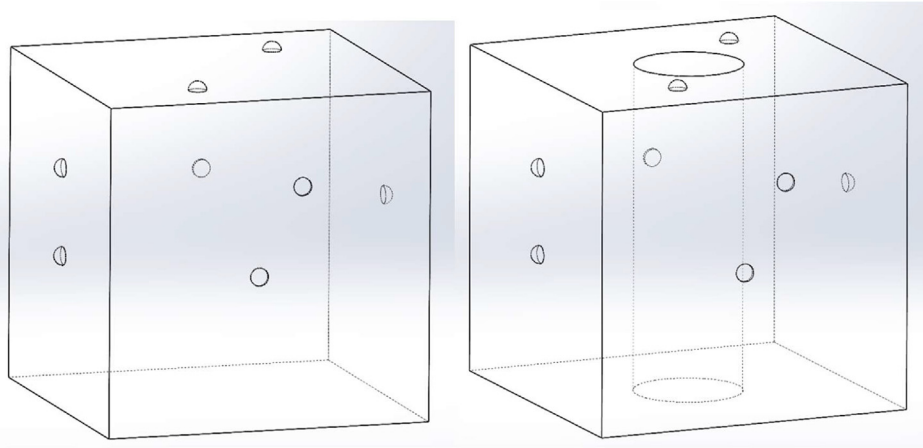


Fig. 3. Location of sensors on cubes a) without the hole and b) with the hole.

- sand to cement ratio is 2.75,
- the water to cement ratio is 0.485.

After moulding, the mixture was vibrated for 4 min for compaction and release of excess air. Samples of 37 mm diameter and 74 mm height were prepared from the same mixture for the UCS test to ensure all blocks were similar in strength as a control measure.

The cube sizes varied between 150 and 450 mm to account for boundary conditions' effect when the holes are introduced and represent increasing mine maturity with time. The cubes were with and without holes. Each hole was in the centre and through the cube's height.

2.2.3. Backfill

The holes in the blocks were filled with different cement to sand ratios to study void content's impact on wave velocity. Backfill ratios of 0% cement (100% dry sand), 0% cement (water-saturated sand), 5% cement, 10% cement, 15% cement, and 20% cement content were used. The different mix ratios represent the different backfill mixes commonly used in the mining industry. Each backfill type was cured to

various ages (8 h, one day, seven days, 14 days, and 28 days). ASTM C-109 C standard was used to establish the ratio of water to dry components, including sand and cement. Clay particles, large fragments, and organic materials were removed through a sieving procedure performed using the AS 200 basic vibratory sieve shaker. All fragments more than 4 mm and less than 0.002 mm were removed as oversized particles and clays, respectively.

2.3. Equipment and testing methods

Acoustic emission testing (AET) is a technique used for the non-destructive testing of materials. AET can track the changes in material behaviour. This technique allows one to observe crack propagations appearing deep inside a material.

Different terms are used to define instabilities or “events” caused by rock fracturing at different scales, as shown in Fig. 4.

CAMIRO [12] notes that in mine seismology, large events in the seismic range are often called mine tremors or mine-induced seismic events. Smaller events, often located close to active mine stopes, are

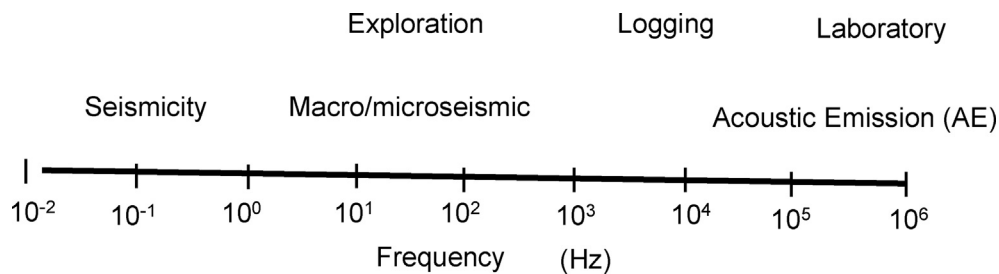


Fig. 4. Monitoring frequency ranges of earthquakes, macro/microseismic activity, acoustic emission, and associated fields of study/research domains [12].

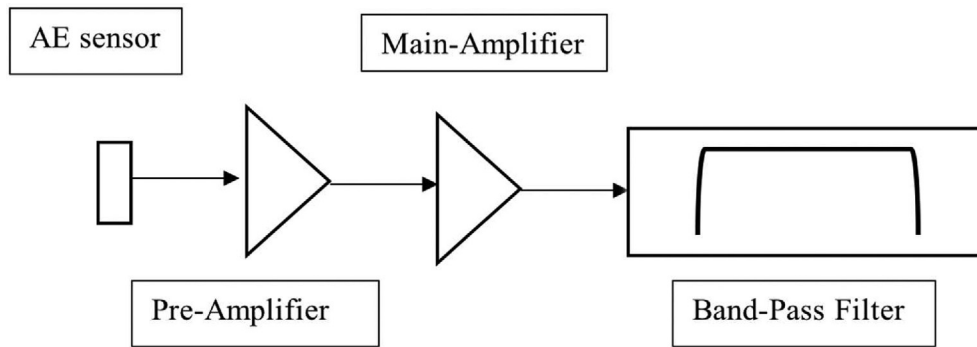
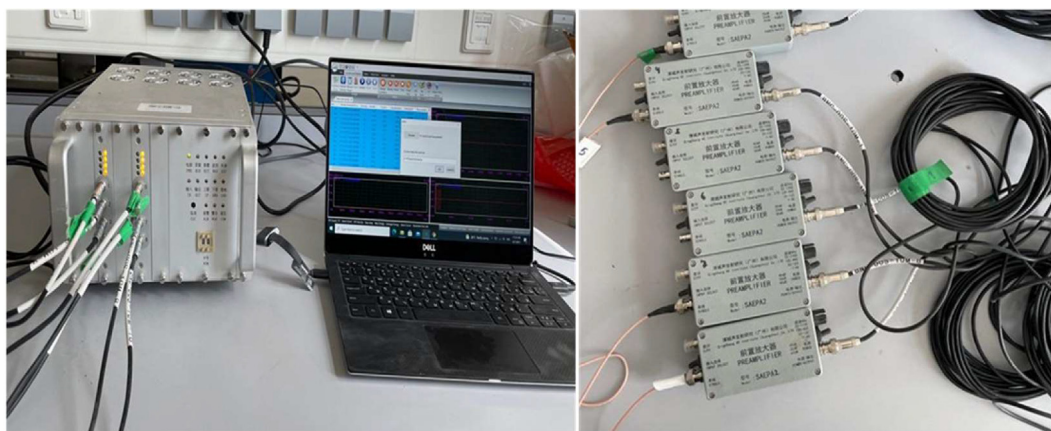


Fig. 5. AE detection system [15].

usually defined as “microseismic events” due to their much smaller magnitudes. At the lowest end of the magnitude spectrum, “acoustic emission” is often used to indicate high-frequency emissions or “rock noise” monitored in rock samples under loading in a laboratory or observed in localized failure areas within a mine. It is known that the boundaries between these different categories are not very well defined, and many authors such as Dong et al. [13] use the term “acoustic emission/microseismic” or simply “AE/MS” to refer to the latter two categories in a general manner. Therefore, microseismicity during the failure process while loading material is very similar to acoustic emission (AE). Acoustic emissions are characterized as the energy released in stressed materials. The release of localized strain energy can be due to fracturing and can be recorded on the material's surface by sensors. Therefore, AET is compared with seismological techniques since they have similar concepts but different scales.

AET has been used to track rock mass defects at the very early stage prior to complete failure. The main difference from other non-destructive tests is the type of data received and the application mechanism. For instance, in the ultrasound method, artificially created signal and source-receiver are used to determine the geometric shape of a defect in a sample. In contrast, AET can determine elastic waves going through fractures in a sample [14]. Compared to other non-destructive methods, AET requires only a few sensors under certain conditions that can have signals passing a trigger level threshold. AET does not need access to all sides of the sample, as is required for all other methods of through-transmission [14].

Fig. 5 illustrates a standard AE detection system. AE sensors transform dynamic motions into electric signals and detect AE waves at a material's surface. A preamplifier and main amplifier are used to increase weak AE signals and could provide more than 1000 times gain.



(a) AE data acquisition modules, chassis with front and rear panels, optional network communication module, laptop

(b) Preamplifiers and cables

Fig. 6. AE system and accessories.

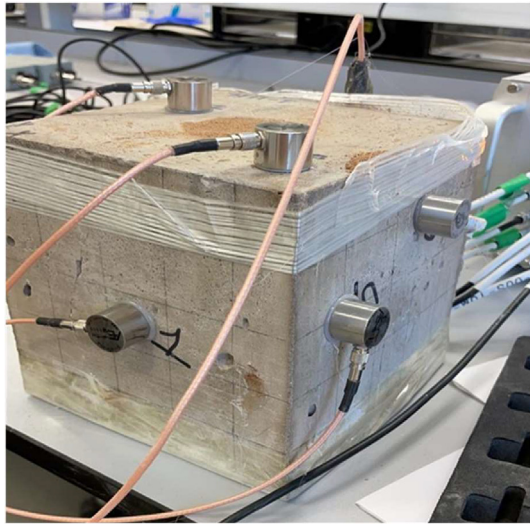


Fig. 7. AE sensors attached to the rock sample.

In Fig. 5, elastic waves generated by the source propagate in the material and are detected by AE sensors [15].

The AE method has been used to study mine seismicity by Dong and Li [16], Ge et al. [17], Kennet et al. [18], and Nivesrangsan et al. [19]. The AE system and accessories are shown in Fig. 6. In this study, the SAEU3H AE system was used. The

SAEU3H AE system is a multi-channel system that consists of AE data acquisition modules, chassis with front and rear panels, an optional network communication module, a laptop, eight sensors, preamplifiers, and cables (Fig. 6).

In the laboratory tests in this research, AE sensors were attached to the surface by hot glue, as shown in Fig. 7. Eight sensors were attached to each cube, with one sensor used as a source that generated a pulse, and the other seven sensors serving as receivers that received the pulse wave. The wave was generated as a pulse from sensor number 1 placed in the middle of the front view of the cube to enable waves to go through the hole.

The sensor used in the experiments for 150 mm, 225 mm, and 300 mm cube sizes is the SR150M high-frequency broadband AE sensor. The frequency range of the sensor is 60–400 kHz; peak sensitivity is > 75 dB. SRI150 sensor type was used for larger cubes of 375 mm and 450 mm. This sensor has a built-in preamplifier with a frequency range of 60–400 kHz and a sensitivity of 40 dB. This change in sensor type was necessitated by the fact that with the SR150M sensors, wave arrival times could not be detected at the receiving sensors due to seismic wave attenuation in inelastic materials such as rocks and concrete materials used in the study. Seismic waves attenuate with time and distance in inelastic

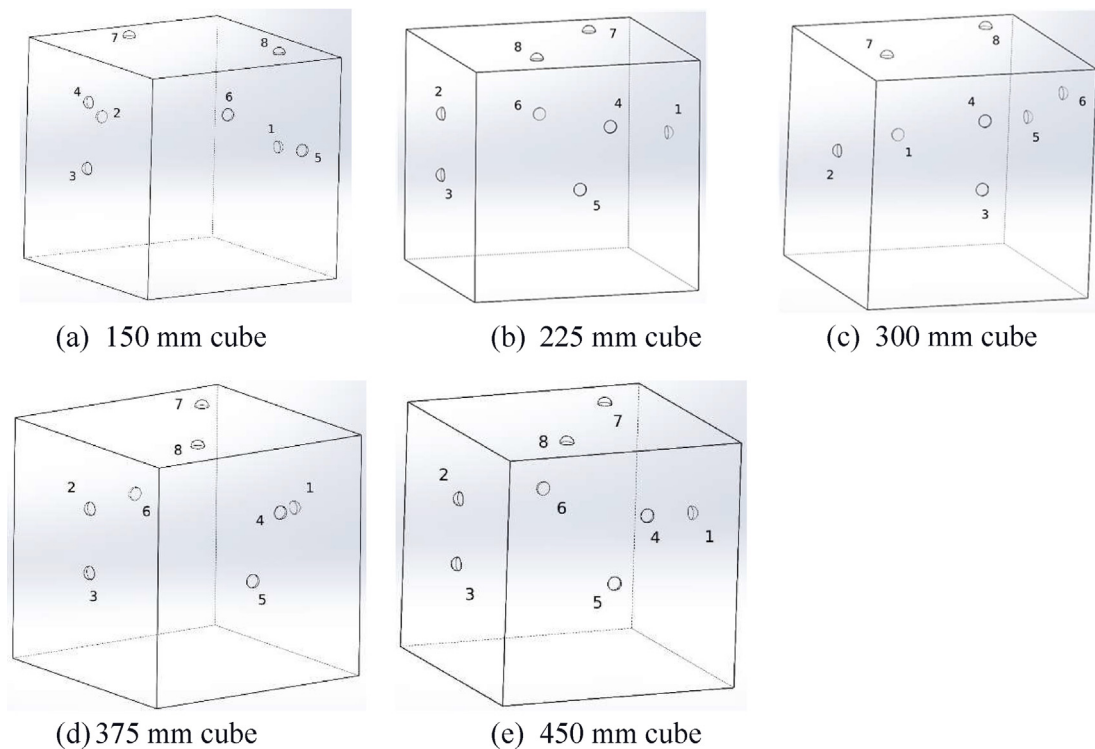


Fig. 8. Sensor positions on the various cube sizes without a hole.

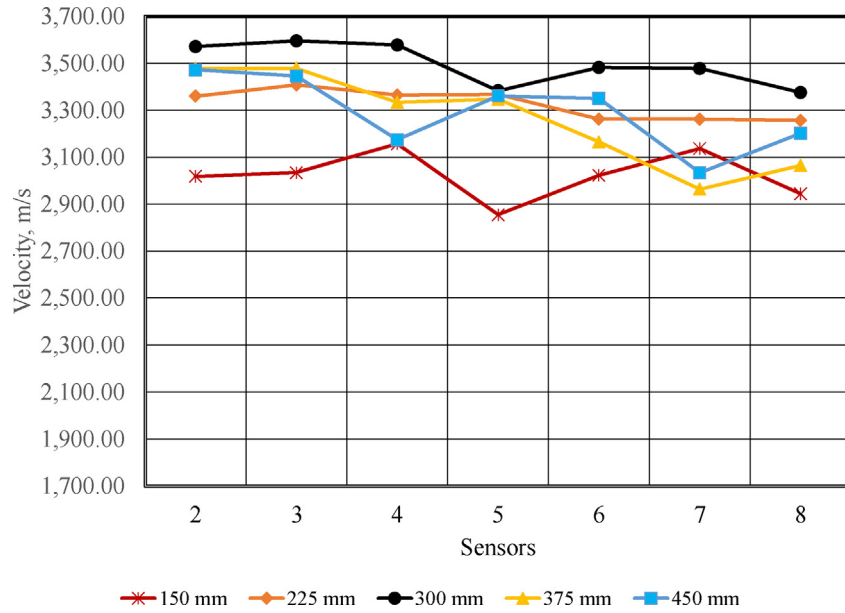


Fig. 9. Seismic wave velocities on concrete cubes without holes.

materials due to various inelastic energy loss mechanisms such as porosity, fractures and microscopic movements along mineral dislocations or shear heating at grain boundaries [20]. According to [20], seismic wave attenuation (ϵ) is often

quantified using a quantity called the quality factor (Q) [Equation (1)].

$$\epsilon = \frac{\gamma}{m\omega_o} = \frac{1}{2Q} \tag{1}$$

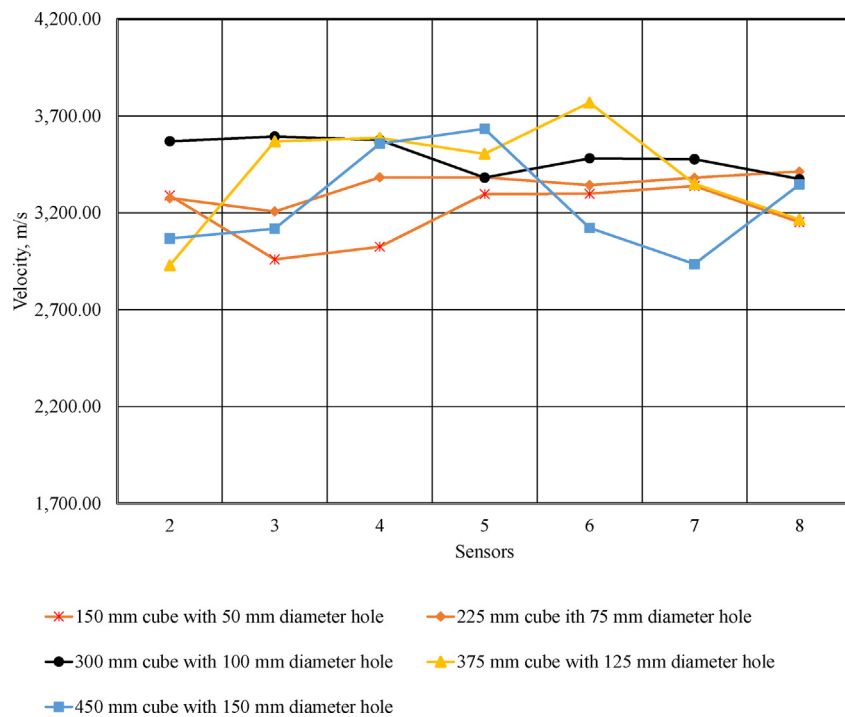


Fig. 10. Seismic wave velocities in blocks with holes of different diameters at sensor locations.

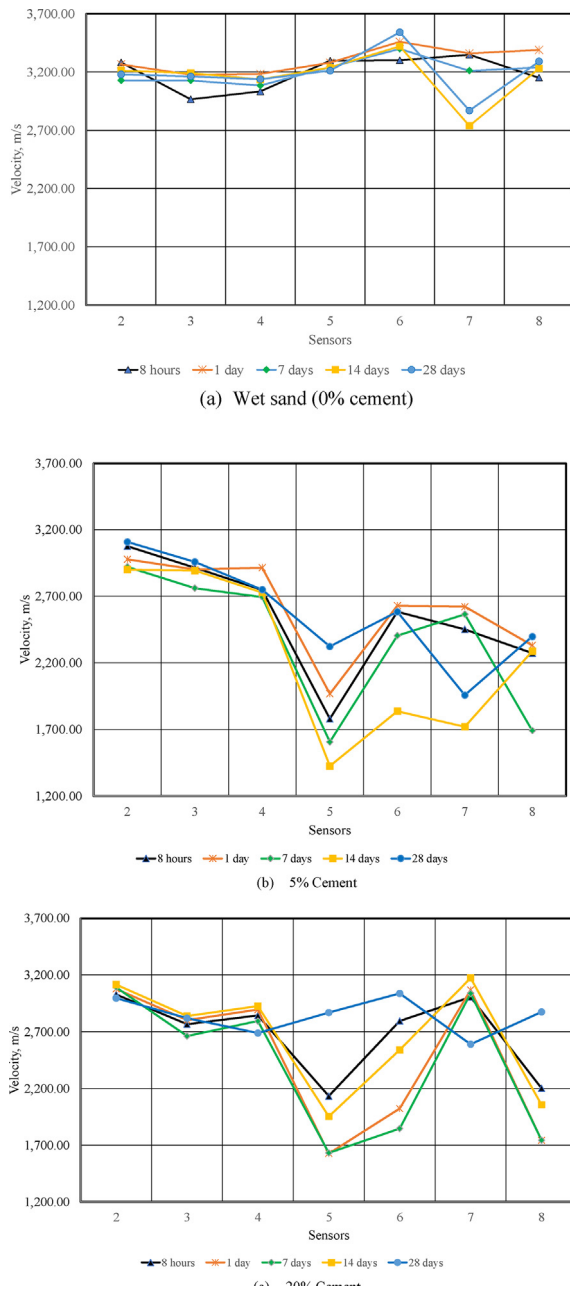


Fig. 11. Backfill effect on seismic wave velocity for 150 mm cube with 50 mm diameter hole (a) Wet sand – 0% cement (b) 5% cement (c) 20% cement backfill.

where γ = coefficient of friction, m = mass and ω_0 = resonant frequency.

A low attenuation (high-quality factor Q) may indicate a tightly bound rock mass or one that can propagate a displacement pulse with little or no energy loss, thus reaching the free surface with nearly full strength, and vice versa. Hence, with the

larger cubes and SR150M sensors, energy loss stopped the wave propagation before they reached the receiving sensors, therefore requiring a change to the SRI150 sensors. CAMIRO [12] notes that the properties of the rock mass affect the way seismic waves propagate through the medium. This influence is not restricted to the velocity of the waves but also includes the relative amplitude and frequency content of the signals referred to as signal degradation or attenuation. In a mining environment, seismic waves propagating through a host medium are affected by the rock type, backfill, voids, state of stress, and the type of structures (faults, shears, and joints) and their distribution.

2.4. Procedure of velocity calculation by AE equipment

Hedley [21] stated that seismic monitoring systems basically measure the arrival times of the seismic waves, and then, knowing the coordinates of the sensors and assuming a uniform velocity at which the seismic signals travel through the rock, an estimate of the source location can be determined. There are two general methods of source location based on the arrival times of the P -waves alone or the arrival times of both the P - and S -waves [21]. In this research, we used the direct method of source locations by Blake, Leighton, and Duvall [22] and discussed in Hedley [21].

Data derived from the AE tests provided the arrival time of the wave at each sensor. Knowing each sensor's arrival times and location coordinates, the distances from the pulse source to the receiving sensor locations were calculated. The corresponding seismic wave velocities were calculated by dividing the distance from the source to each sensor by the wave arrival time at the sensor.

The use of the AE procedure to determine the arrival time of the wave generated by the source sensor pulse includes the following steps:

1. Construction of coordinate system with grid and coordinate values on the surfaces of blocks.
2. Sensor placement around the samples at known coordinate points; the test should include at least four sensors along the different lines.
3. One of the eight sensors used as a source, while the other sensors were receivers.
4. The eight-channel SAEU3H acoustic emission system was used to collect source location and arrival times. Each cube with a drill hole had a control sample without a hole.

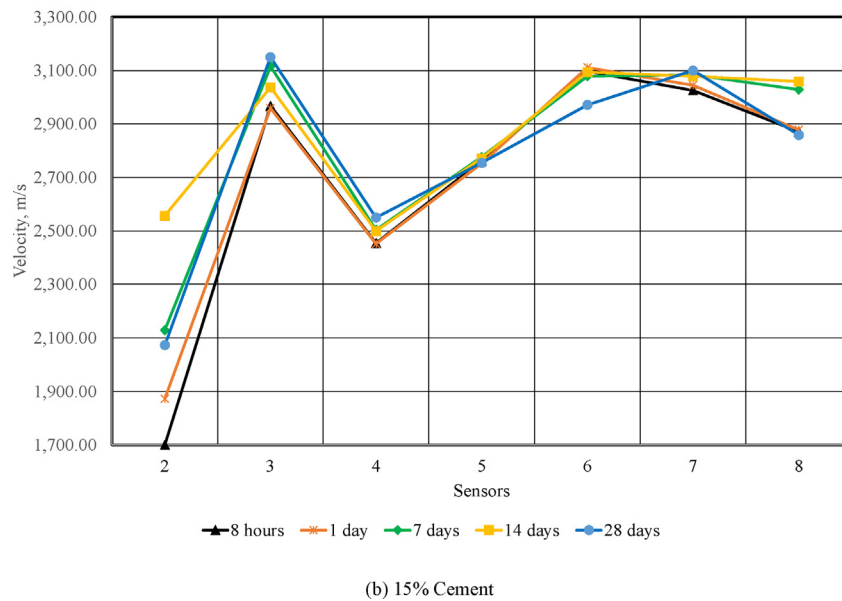
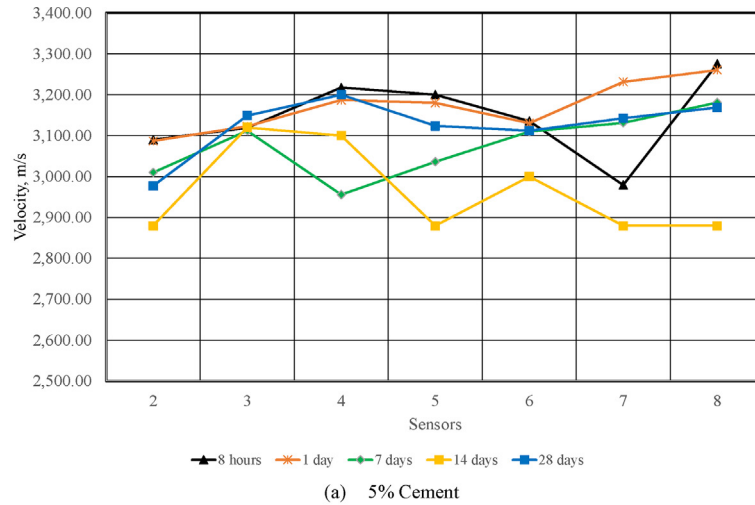


Fig. 12. Backfill effect on seismic wave velocity for 225 mm concrete cube with 75 mm diameter hole (a) 5% cement (b) 15% cement.

5. Based on the coordinates and wave arrival times, the wave velocity to each sensor was calculated.

Figure 8 shows the sensor positions in the various block sizes used. These blocks are without the central holes representing volumes of extraction with increasing mine life.

Following the procedure developed by Blake, Leighton, and Duval [22], the distance between the source and receiving sensors was calculated according to Equation (1):

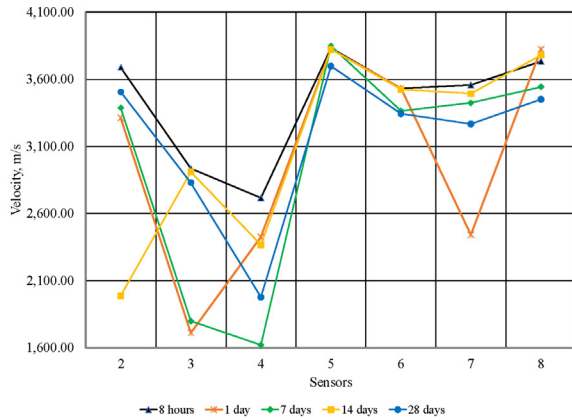
$$d_i = \sqrt{(x_i - x_1)^2 + (y_i - y_1)^2 + (z_i - z_1)^2} \tag{2}$$

where $i = 2, 3, 4, 5, 6, 7, 8$ and x, y, z – sensor coordinates.

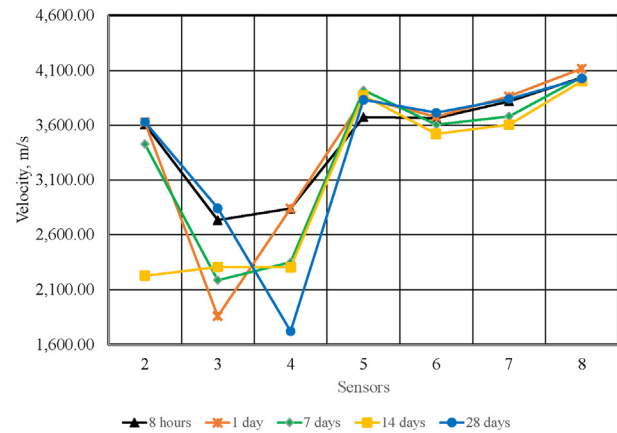
Wave velocity was calculated by the following equation, by dividing the distance of each sensor from the source by its corresponding wave arrival time:

$$v = \frac{d_i}{\Delta t} \tag{3}$$

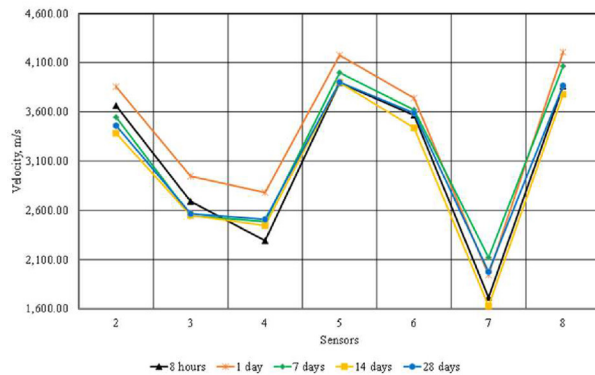
In Equation (3) d_i is the distance of each sensor 2, 3, 4, 5, 6, 7, 8 from the source at x_1, y_1, z_1 , and Δt is the wave arrival time from the source.



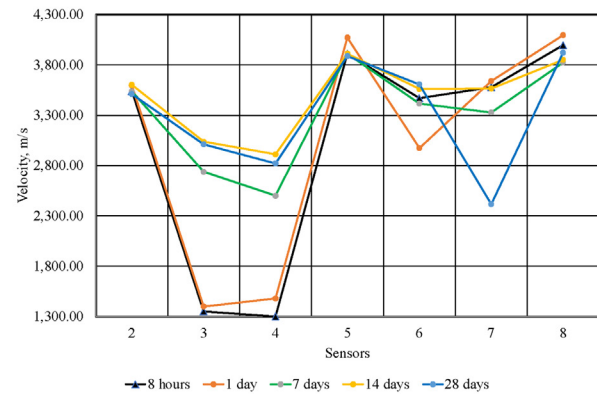
(a) Wet sand – 0% cement



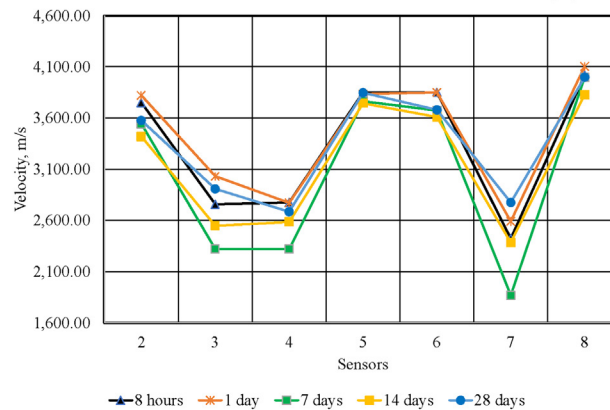
(b) 5% Cement



(c) 10% Cement



(d) 15% Cement



(e) 20% Cement

Fig. 13. Backfill effect on seismic wave velocity for 300 mm granite cube with 100 mm diameter hole (a) Wet sand – 0% cement (b) 5% cement (c) 10% cement (d) 15% cement (e) 20% cement.

The procedure described for the distance calculations assumes the material is homogeneous and without voids or fractures to affect the wave path (i.e., the procedure assumes the so-called straight ray path concept [23,24].

3. Results and discussion

3.1. Size effect on seismic wave velocity

The primary purpose of the research was to see the effect of size, voids, and different backfill content

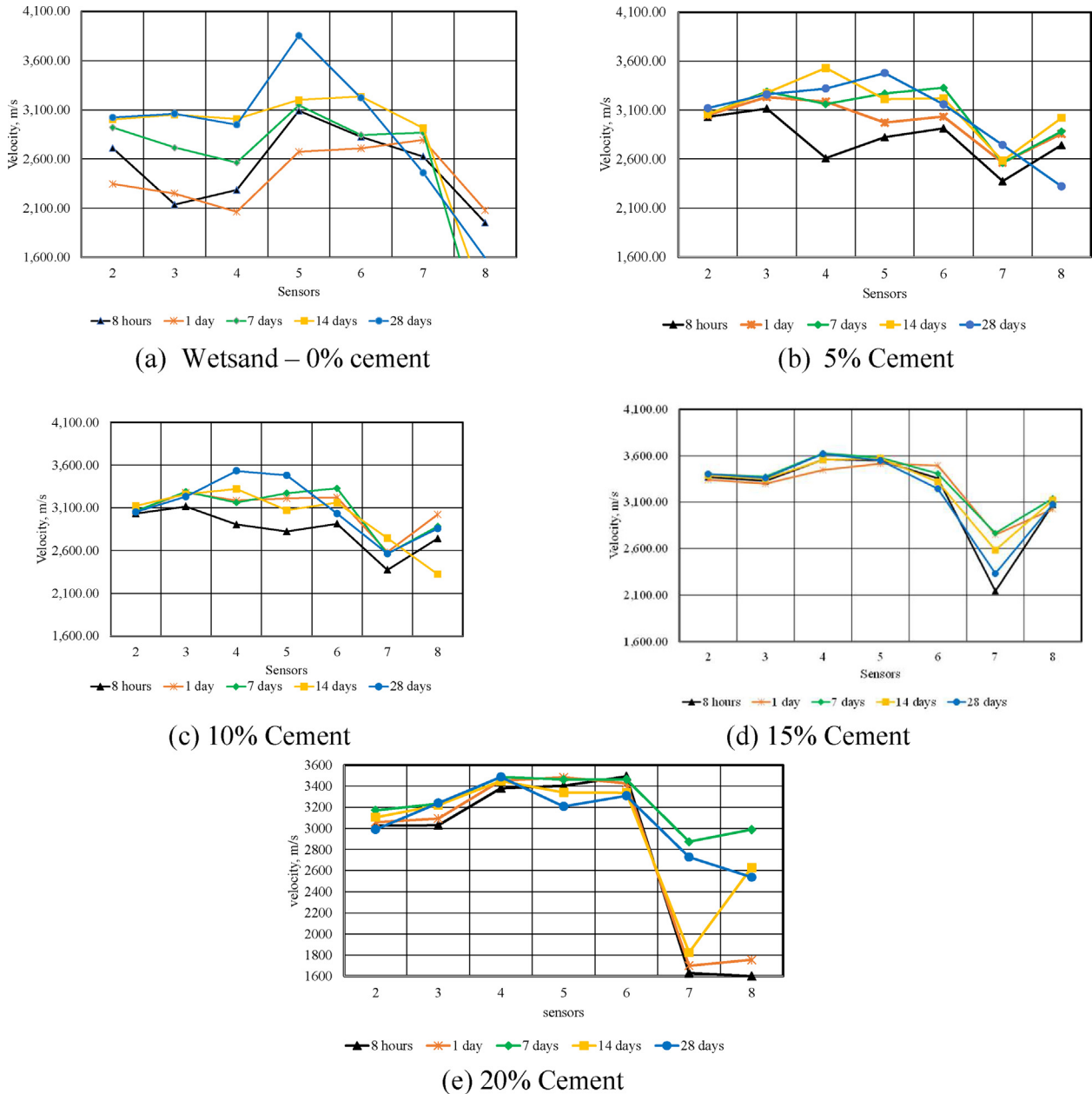


Fig. 14. Backfill effect on seismic wave velocity for 375 mm concrete cube with 125 mm diameter hole (a) wet sand (b) 5% cement (c) 10% cement (d) 15% cement (e) 20% cement backfill.

and age on seismic wave velocity. AE tests were repeated five times for each cubic sample. Fig. 9 shows seismic wave velocities for cubes of all sizes without holes. An average of 5 velocity measurements was used at each sensor to plot the graph. Based on the test results shown in Fig. 9, except at sensor 7, there is no significant difference in seismic wave velocities with increasing cube size. The range of wave velocities of between 3000–3500 m/s is within the values of 3160–3818 m/s with a standard deviation of 146 m/s determined by Lee and Oh [25].

The smaller cube of 150 mm diameter shows the lowest velocities at the sensors with the least velocity of 2855 m/s at sensor 5. The small variations in the velocities for all five cubes could be from the concrete mix quality variations and possible errors in the determination of the wave arrival times.

3.2. Hole effect on seismic wave velocity

Fig. 10 shows the results of AE tests on concrete cubes with empty holes. The hole diameter

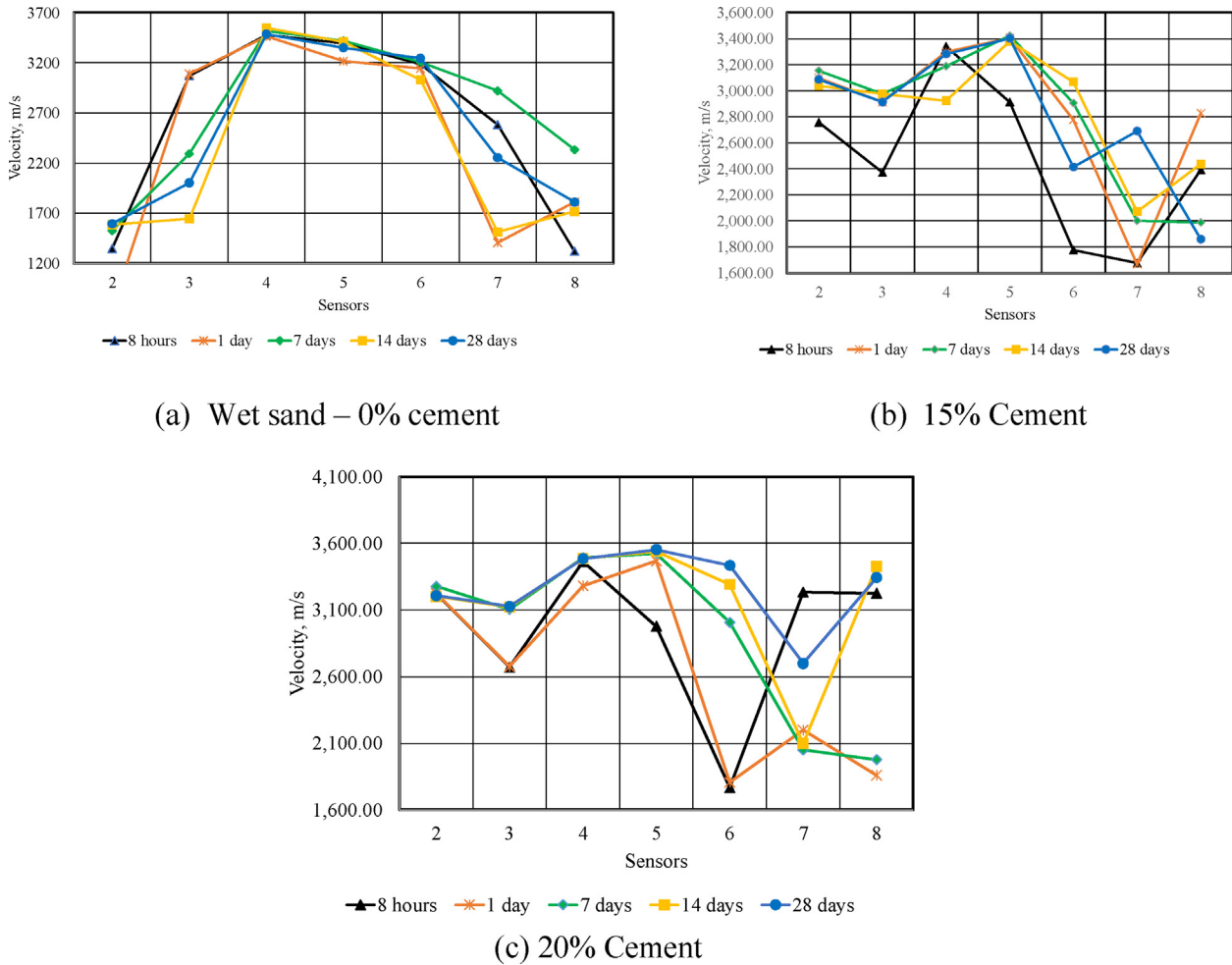


Fig. 15. Backfill effect on seismic wave velocity for 450 mm concrete cube with 150 mm diameter hole (a) wet sand (b) 15% cement (c) 20% cement backfill.

increases with increasing cube size. According to the test results in Fig. 10, the velocities in the 150-, 225-, 300- and 375-mm cubes with holes of 50-, 75-, 100- and 125-mm diameters are not significantly affected compared with their equivalent cubes without holes. For these cubes, the velocities at the sensors range between 3033 and 3577 m/s. The cube size of 450 mm with a hole diameter of 150 mm shows a significant change in the seismic wave velocity at sensors 2, 3, 6 and 7. Sensors 4 and 5 show relatively higher velocities of 3558 and 3635 m/s, respectively, implying that they are not affected by the void. Sensors 6 and 7 show the most significant drop in velocities of almost 1500 m/s from the peak value in the 450 mm cube with a hole diameter of 150 mm. The significant drop in velocities is caused by the sensors' location across the hole from the

source sensor. Wave energy attenuation is high due to the empty 150 mm diameter hole and the effect of ray path tracing that is ignored in the distance calculation, resulting in longer arrival time and, therefore, lower velocities. The results show that ray paths being assumed straight in this case were not significantly affected by the holes in the smaller cubes but were impacted by the hole diameter of 150 mm in the 450 mm cube with the severity depending on the sensor location relative to the source and hole.

3.3. Backfill effect on seismic wave velocity

The effect of backfill at different ages in the holes of the blocks can be related to the effect of a layered velocity model as opposed to the uniform velocity

model (straight ray paths from source) according to the Fermat principle. In the layered velocity model, the ray path from the source is a polyline with an inflection at the interface of the layers [23]. Based on these principles, waves travelling in the concrete through the backfill material will have their velocities impacted.

Fig. 11 shows seismic wave velocity results for each backfill type at cured age for wet sand (0% cement), 5% and 20% cement, respectively, for a cube size of 150 mm with a hole diameter of 50 mm. Based on the positions of sensors 2, 3, 4 and 5 in Fig. 11a for wet sand, the ray paths of these sensors are not impacted by the backfill in the void, while the ray paths from the source to sensor 7 are significantly impacted by the void and its contents in days 14 and 28 when the wet sand would have been dry. For the higher cement content backfill (15% and 20% cement), there is less impact on the wave velocity at 28 days of curing time, as can be seen in Fig. 11c. In Fig. 11b, there is a general decrease in velocities for all curing times at sensors 5 to 8 that is attributed to the void and its content and the locations of these sensors relative to the source. Fig. 11c, with a backfill cement content of 20%, shows the significant impact of the void and its content on the pulse wave velocities at sensors 5, 6 and 8 because of their relative locations to the void and source. It is reasonable to say that, even though straight ray paths were assumed in the pulse wave velocity calculations, the impact of the void and its contents is visible without ray tracing but could be better with ray tracing.

Fig. 12 shows the impact of the void and backfill effect on wave velocities at the receiving sensors on the 225 mm cube with 5% and 15% cement content backfill in the void. In Fig. 12a, for 5% cement content backfill, the wave velocities for all the cured times fall within the range of 2879–3200 m/s, like in a homogeneous material. The pulse wave velocity is significantly affected from the source to the receiving sensors 2 and 4 in Fig. 12b because of the void and backfill, as can be seen in Fig. 12a (wet sand).

Fig. 13 shows the AE test results for the 300 mm granite cube with different cement content backfills at different ages. Fig. 13 a, c and e show drops in velocities at sensors 3, 4 and 7, which reflect their relative locations to the source and void. The velocities at the other sensors are not impacted. This implies that their ray paths were not affected by the void. Velocities at sensors 2, 5, 6 and 8 are not impacted and fall in the range of 3600–4100 m/s.

According to Fig. 14, sensors 7 and 8 are significantly affected by the void of 125 mm diameter and changes in backfill properties with time in the

375 mm cube. The two sensors are located at the top of the cube near the void, and wave paths to these sensors are impacted by the void and its contents to different degrees.

Fig. 15 shows the results of the impact of back-filled cement content with time on wave velocities at sensors attached to the 450 mm cubes with a void of 150 mm diameter at different locations relative to the source and void. In Fig. 15a for wet sand with 0% cement, the velocities show lower values at sensors 2, 3, 7 and 8. This is due to the sensor locations relative to the void and source.

4. Conclusions

Input velocity models in seismic monitoring systems algorithms for seismic event source locations determination affect the accuracy of the source locations in underground mining environments. Uniform velocity models assume rock masses are homogeneous. Layered velocity models, on the other hand, ignore the effect of other factors, such as voids and fractures. Recent works using 3D Velocity models and ray path tracing have shown significant improvements to seismic event source location accuracies.

Establishing a reliable velocity model in mining is a challenge, as multiple rock types are encountered, and the rock mass conditions are constantly changing due to the creation of voids that may or may not be backfilled, and stress changes that cause continuous fracturing of the rock mass. The consequence of the changing ground condition, coupled with the existence of multiple rock types and backfills, is a continuously changing velocity model (CCVM) contrary to the assumption of single (homogeneous rock mass assumption) or variable static constant velocity models (layered rocks assumption), currently used in seismic monitoring systems for the calculation of seismic source locations. One strategy often used to account for changing ground conditions in the velocity model is periodic updating of the velocity. This approach is not only cumbersome but time consuming, and most importantly event source locations in between the periodic updates will not be reliable.

The objective of this research is to develop novel means for tracking velocity changes in continuously degrading ground conditions due to mining activities in underground mining environments, for the purpose of selecting the appropriate velocity for source location calculations in seismic monitoring systems in real time.

The approach adopted in the research involves the use of discrete physical models as analogues to

mimic the changing ground conditions in underground mining to capture the impact on seismic wave velocity. In the discrete physical modelling concept, rather than using a single block and changing its condition to reflect the constantly changing ground condition in mining environments (a physically challenging approach), separate individual blocks are used, with each block representing a different stage in the mining process in time, structure, and geometry.

While the study did not explicitly use the concept of ray tracing to account for travel ray path changes due to voids, the results clearly show the impact of voids and their contents on the pulse wave velocities using acoustic emission (AE) monitoring systems.

The results also show that while the straight seismic ray path method was used, depending on sensor location relative to the pulse event source, the impact of the void and its content with time were clearly visible, confirming that in mining where ground conditions are constantly changing a uniform constant or periodically changing velocity model is not appropriate for accurate seismic event source locations.

The research is ongoing and will include the effect of stress and blast-induced fracturing on the seismic wave velocity model. Eventually, machine learning (ML) or artificial intelligence (AI) will be applied to the data to enable real-time velocity prediction for use in seismic event source calculation algorithms in seismic monitoring systems for improved accuracy in seismic event source locations.

Ethical statement

The authors state that the research was conducted according to ethical standards.

Conflict of interest

The authors declare no conflict of interest.

Funding body

The authors acknowledge Nazarbayev University for support through the Collaborative Research Program Grant # OPCR2020014.

References

- [1] Palei SK, Das SK. Logistic regression model for prediction of roof fall risks in bord and pillar workings in coal mines: an approach. *Saf Sci* [Internet]. Elsevier 2009;vol. 47:88–96. Available from: <https://doi.org/10.1016/j.ssci.2008.01.002>.
- [2] Fall M, Célestin JC, Pokharel M, Touré M. A contribution to understanding the effects of curing temperature on the mechanical properties of mine cemented tailings backfill. Elsevier B.V. *Eng Geol Invest* 2010;114:397–413. Available from: <https://doi.org/10.1016/j.enggeo.2010.05.016>.
- [3] Shi X, Jing H, Yin Q, Zhao Z, Han G, Gao Y. Investigation on physical and mechanical properties of bedded sandstone after high-temperature exposure. *Bull Eng Geol Environ. Bulletin of Engineering Geology and the Environment* 2020; 79:2591–606.
- [4] Ranjith PG, Zhao J, Ju M, De Silva RVS, Rathnaweera TD, Bandara AKMS. Opportunities and challenges in deep mining: a brief review. Elsevier LTD on behalf of Chinese Academy of Engineering and Higher Education Press Limited Company Engineering 2017;vol. 3:546–51. Available from: <https://doi.org/10.1016/J.ENG.2017.04.024>.
- [5] Xie H, Gao F, Ju Y. Research and development of rock mechanics in deep ground engineering. *Yanshilixue Yu Gongcheng Xuebao/Chinese J Rock Mech Eng.* 2015;34: 2161–78.
- [6] Collins DS, Pinnock I, Toya Y, Shumila V, Trifu CI. Seismic event location and source mechanism accounting for complex block geology and voids. 48th US Rock Mech/Geomech Symp. 2014;1:63–9.
- [7] Trifu CI, Shumila V. Geometrical and inhomogeneous ray-path effects on the characterization of open-pit seismicity. 44th US Rock Mech Symp - 5th US/Canada Rock Mech Symp; 2010.
- [8] Vilhelm J, Ivankina T, Lokajčiček T, Rudajev V. Comparison of laboratory and field measurements of P and S wave velocities of a peridotite rock. *Int J Rock Mech Min Sci* 2016;88: 235–41.
- [9] Wulff AM, Raab S, Huenges E. Alteration of seismic wave properties and fluid permeability in sandstones due to microfracturing. *Phys Chem Earth, Part A Solid Earth Geod* 2000;25:141–7.
- [10] Memon RP, Sam ARM, Awang AZ, Memon UI. Effect of improper curing on the properties of normal strength concrete. *Eng Technol Appl Sci Res* 2018;8:3536–40.
- [11] C109/109M-16a A. Standard test method for compressive strength of hydraulic cement mortars (Using 2-in. or cube specimens). *Annu Book ASTM Stand* 2016:1–10.
- [12] CAMIRO. Canadian rockbursts handbook6 Volumes. Mining Research Directorate; 1996.
- [13] Dong L, Sun D, Li X, Du K. Theoretical and experimental studies of localization methodology for AE and microseismic sources without pre-measured wave velocity in mines. 2017. See, http://www.ieee.org/publications_standards/publications/rights/index.html for more information.
- [14] Yassin A. ENGR 489: NDT Spring 2020 Acoustic emission testing (AET) submitted by : students' name supervised by: instructor: Dr . Ameen El Sinawi. 2020. 0–vol. 33.
- [15] Grosse CU, Masayasu Ohtsu, Aggelis DG, Shiotani T. Acoustic emission testing basics for research – applications in engineering [Internet]. Springer; 2022. Available from: <http://www.springer.com/series/15088>.
- [16] Dong L, Li X. A microseismic/acoustic emission source location method using arrival times of PS waves for unknown velocity system, 2013 using arrival times of PS waves for unknown velocity system. *Int J Distributed Sens Netw* 2013;2013:8. <https://doi.org/10.1155/2013/307489>. Article ID 307489.
- [17] Ge M, Hardy Jr HR, Wang H, Wang J. Development of a simple mechanical impact system as a non-explosive seismic source. *Geotech Geol Eng* 2011;29(1):137–42.
- [18] Kennett BLN, Marson-Pidgeon K, Sambridge MS. Seismic source characterization using a Neighbourhood Algorithm. *Geophys Res Lett* 2000;27(20):3401–4.
- [19] Nivesrangan P, Steel JA, Reuben RL. Source location of acoustic emission in diesel engines. *Mech Syst Signal Process* 2007;21(2):1103–14.
- [20] Ammon CJ, Velasco AA, Lay T, Wallace TC. Foundations of seismology. 2nd ed. Academic Press; 2021.

- [21] Hedley DGF. Rockburst handbook for ontario hardrock mines. CANMET special report SP92-1E. 1992.
- [22] Blake W, Leighton FW, Duvall W. Microseismic techniques for monitoring the behaviour of rock structures. Bull (Arch Am Art) 1974;vol. 665. U.S. Bureau of Mines.
- [23] Peng P, Jiang Y, Wang L, He Z, Tu S. Mining-induced seismicity by considering underground voids. 2020. <https://doi.org/10.3390/app10196763>.
- [24] Morkel IG, Wesseloo J, Potvin Y. Seismic event location uncertainty in mining with reference to caving. Adelaide, Australia: Cave2022; 2022.
- [25] Lee YH, Oh T. The measurement of P-, S-, and R-wave velocities to evaluate the condition of reinforced and prestressed concrete slabs. Adv Mater Sci Eng 2016;2016:14p. <https://doi.org/10.1155/2016/1548215>.